

INVESTIGATION OF THE $^{24}\text{Mg}(\alpha, \gamma)^{28}\text{Si}$ REACTION AND OF SOME $^{27}\text{Al}(p, \gamma)^{28}\text{Si}$ RESONANCES

by P. J. M. SMULDERS and P. M. ENDT

Fysisch Laboratorium der Rijksuniversiteit, Utrecht, Nederland

Synopsis

The yield of 8–13 MeV γ radiation from the $^{24}\text{Mg}(\alpha, \gamma)^{28}\text{Si}$ reaction has been measured in the $E_\alpha = 1.2\text{--}3.2$ MeV range, making use of natural Mg and enriched ^{24}Mg targets. Twenty resonances were observed, corresponding to ^{28}Si levels in the $E_x = 11.3\text{--}12.8$ MeV region. Six resonances show a relatively strong ground-state transition (γ_0); the spin and parity (either 1^- , or 2^+) of these resonances was uniquely determined through angular distribution measurements. At nine other resonances the angular distribution was measured of γ_1 , the transition to the ^{28}Si first excited state at 1.77 MeV; supplemented with angular correlation measurements in several different geometries, this uniquely determined the J^π of these resonances. The remaining five resonances are weak.

The strongest resonances have $J^\pi = 2^+$ or 4^+ . These are deexcited through $E2$ or strongly mixed $M1\text{--}E2$ transitions.

In both the $^{24}\text{Mg}(\alpha, \gamma)^{28}\text{Si}$ and $^{27}\text{Al}(p, \gamma)^{28}\text{Si}$ reactions a level in ^{28}Si at $E_x = 12.24$ MeV is excited. The (unique) spin determinations from these reactions, however, do not agree, yielding $J^\pi = 4^+$ and $J^\pi = 3^+$, respectively. Although the γ -ray single spectra are closely analogous, pronounced differences exist in the $\gamma\text{--}\gamma$ coincidence spectra measured from the two reactions, showing that actually two closely spaced ($\Delta E_x \approx 0.6$ keV) levels in ^{28}Si are excited.

A new, extremely weak, resonance in the $^{27}\text{Al}(p, \gamma)^{28}\text{Si}$ reaction has been observed at $E_p = 202.3 \pm 0.9$ keV.

The data obtained from the $^{24}\text{Mg}(\alpha, \gamma)^{28}\text{Si}$ reaction are compared with the information from the $^{27}\text{Al}(p, \gamma)^{28}\text{Si}$ and $^{27}\text{Al}(p, \alpha)^{24}\text{Mg}$ reactions. From the measured yields of these three reactions, the partial widths Γ_α , Γ_p and Γ_γ are computed for most resonance levels.

1. *Introduction.* The alpha-particle capture reaction has, apparently, been neglected as a spectroscopic tool. The only published information concerns capture in $1p$ -shell nuclei¹⁾. A very attractive feature of this reaction is the fact that the α particle is spinless, which entails a considerable simplification in the interpretation of angular correlation measurements. The main obstacle in (α, γ) work is the prolific neutron production, primarily through the $^{13}\text{C}(\alpha, n)^{16}\text{O}$ reaction, always accompanying the acceleration of helium ions. Capture of these neutrons in the NaI scintillation crystals used for γ -ray detection, results in a formidable background extending to about $E_\gamma = 8$ MeV.

The foregoing discussion implies that the investigation of a particular (α, γ) reaction is difficult unless the energy of the γ radiation produced is above 8 MeV. A second requirement is that the compound nucleus should not be neutron unstable. In the $2s-1d$ shell these requirements are met e.g. for capture in ^{20}Ne , ^{24}Mg , ^{28}Si , ^{30}Si , ^{32}S , and ^{34}S . All these reactions which have the additional advantage that the initial nucleus is also spinless, have been or are investigated in Utrecht. The present paper only deals with the $^{24}\text{Mg}(\alpha, \gamma)^{28}\text{Si}$ reaction.

The latter reaction was singled out because, first, it has the highest Q value (9.986 MeV) of the reactions mentioned above. With a 3 MeV Van de Graaff generator the region of excitation in ^{28}Si between $E_x = 11$ and 13 MeV can be investigated. Both ground-state transitions (γ_0), and transitions to the first excited state at $E_x = 1.77$ MeV (γ_1) extend in energy well above the neutron background. Second, it was hoped that the $^{24}\text{Mg}(\alpha, \gamma)^{28}\text{Si}$ reaction might supply more information on ^{28}Si resonant states, which in Utrecht already extensively had been investigated by means of the $^{27}\text{Al}(p, \gamma)^{28}\text{Si}$ ²) and $^{27}\text{Al}(p, \alpha)^{24}\text{Mg}$ ³) reactions. Knowledge of the thick target yields for resonant states seen in all three reactions, should make it possible to obtain the partial widths of these states, Γ_α , Γ_p , and Γ_γ .

Two reports have been published of the preliminary results of the present work⁴).

2. Angular correlation analysis. Information on spins and parities of ^{28}Si resonant states is obtained through measurements of the γ_0 and/or γ_1 angular distributions. This can be supplemented with measurements of the angular correlation of the two γ rays forming the cascade through the first excited state.

If the angular distribution of γ_0 can be measured the situation is very simple. Capture of the spinless α particle in a spinless initial nucleus leads to a resonant state of natural parity ($J^\pi = 0^+, 1^-, 2^+$ etc.). The observation of γ_0 then limits the possibilities to $J^\pi = 1^-$ or 2^+ . Resonant states with $J = 0$ or $J > 2$ would not decay to $^{28}\text{Si}(0)(J^\pi = 0^+)$, but to $^{28}\text{Si}(1)(J^\pi = 2^+)$ or to higher levels. Theoretically, the γ_0 angular distributions for $J^\pi = 1^-$ and 2^+ are given by⁵):

$$W(\vartheta) \sim \sin^2 \vartheta \sim 1 - P_2(\cos \vartheta) \quad (J^\pi = 1^-),$$

and

$$W(\vartheta) \sim \sin^2 2\vartheta \sim 1 + \frac{5}{7}P_2(\cos \vartheta) - \frac{12}{7}P_4(\cos \vartheta) \quad (J^\pi = 2^+).$$

The $P_2(\cos \vartheta)$ and $P_4(\cos \vartheta)$ are Legendre polynomials. In fig. 1a it is shown that these angular distributions are very pronounced and completely different. The simplicity of these expressions stems from the fact that no channel spin mixing, orbital momentum mixing, or radiation mixing is possible.

The γ_1 angular distribution generally does not yield such direct and unique information. The possibilities to be considered for the resonant state are $J^\pi = 0^+, 1^-, 2^+, 3^-$, or 4^+ . The angular distribution of the $0^+ \rightarrow 2^+$ transition to $^{28}\text{Si}(1)$ is isotropic; the $4^+ \rightarrow 2^+$ angular distribution is also simple because $E2-M3$ mixing is regarded as highly improbable. These two unmixed cases are shown in fig. 1b. The probability of the occurrence of $E1-M2$ mixing has in the past also been regarded as quite small. Recently however, some cases have been brought forward in which it was shown without doubt that such mixing has to be taken into account³²). The corresponding $J^\pi = 1^-$ and 3^- cases are shown in Figs. 1c and 1e, respectively, for different values of the amplitude mixing parameter κ . For the $2^+ \rightarrow 2^+$

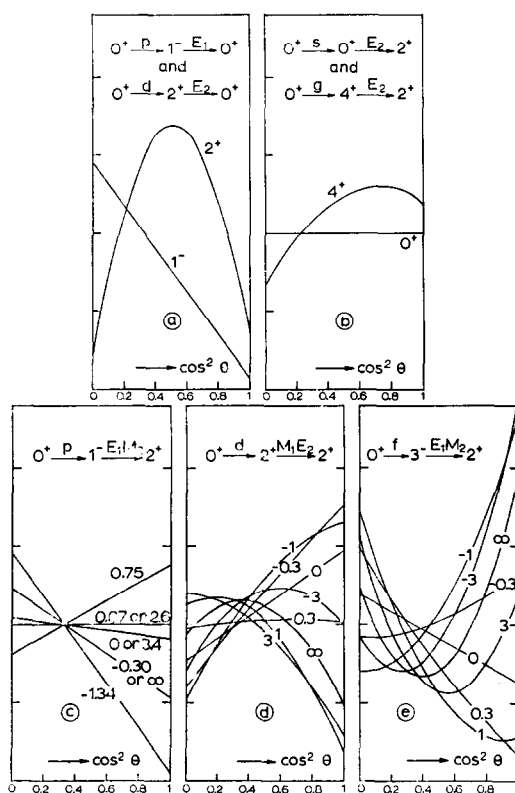


Fig. 1. Theoretical angular distributions of γ radiation following α -particle capture in even-even nuclei.

- Angular distribution of γ_0 , resonance J^π is 1^- or 2^+ .
- Angular distribution of γ_1 , resonance J^π is 0^+ or 4^+ .
- Angular distribution of γ_1 , resonance J^π is 1^- .
- Angular distribution of γ_1 , resonance J^π is 2^+ .
- Angular distribution of γ_1 , resonance J^π is 3^- .

The parameter in c), d) and e) represents the quadrupole-dipole amplitude mixing parameter κ . Solid angle attenuation factors $Q_2 = 0.93$, $Q_4 = 0.76$ have been applied.

case (fig. 1*d*), $M1-E2$ radiation mixing is, of course, quite plausible. The theoretical expressions for the cases treated above, are given in table I⁵⁾.

TABLE I

Angular distribution coefficients of the transition to the ^{28}Si first excited state ($J^\pi = 2^+$) in the expression: $W(\vartheta) \sim 1 + A_2 P_2(\cos \vartheta) + A_4 P_4(\cos \vartheta)$ ^{a)} .		
Transition	A_2	A_4
$E2$ $0^+ \longrightarrow 2^+$	0	0
$E1 + M2$ $1^- \longrightarrow 2^+$	$\frac{-1/10 + 3/5\sqrt{5}x - 1/2x^2}{1 + x^2}$	0
$M1 + E2$ $2^+ \longrightarrow 2^+$	$\frac{+1/2 - \sqrt{15/7}x - 15/68x^2}{1 + x^2}$	$\frac{-24/49x^2}{1 + x^2}$
$E1 + M2$ $3^- \longrightarrow 2^+$	$\frac{-2/5 - 2\sqrt{6/5}x + 1/7x^2}{1 + x^2}$	$\frac{+6/7x^2}{1 + x^2}$
$E2$ $4^+ \longrightarrow 2^+$	$+25/49$	$-18/49$

a) The sign of the amplitude mixing ratio has been chosen in accordance with the Ferguson and Rutledge tables ⁶⁾.

From fig. 1, it is clear that only in rare cases the γ_1 angular distribution is able to yield an unambiguous determination of the resonant state J^π . In particular, the angular distributions for the unmixed $0^+ \rightarrow 2^+$, $1^- \rightarrow 2^+$, and $4^+ \rightarrow 2^+$ transitions can be closely simulated by a $2^+ \rightarrow 2^+$ transition with properly chosen $M1-E2$ radiation mixing.

In these cases, generally, a unique solution can only be found by also performing $\gamma-\gamma$ triple angular correlation measurements. Four standard geometries have been used, indicated as I, II, V, and VI. One counter rotates in a horizontal plane at angles between $\vartheta = 0^\circ$ and 90° with the α -particle beam (the beam being assumed to come in horizontally). The other counter is fixed perpendicular to the beam, either in the horizontal plane (geometries I and II), or vertically above the target (geometries V and VI). In geometries I and V the first γ ray of the cascade is detected in the rotating counter, in geometries II and VI it is detected in the fixed counter. The theoretical expressions for these cases again may be written in the form $W(\vartheta) \sim 1 + A_2 P_2(\cos \vartheta) + A_4 P_4(\cos \vartheta)$; the A_2 and A_4 coefficients were calculated using the Ferguson and Rutledge tables⁶⁾. The $J^\pi = 4^+$ case, however, can only be found from the tables by Sharp *et al.*⁵⁾, with considerably more computational labour.

3. *The yield curve.* Singly charged helium ions have been accelerated with the Utrecht Van de Graaff generator up to energies of 3.2 MeV. The current,

varying between 3 and 8 μA , was largest at the higher energies. The energy was determined with a 90° deflecting magnet, in which the orbit radius amounted to 31 cm. The magnetic field was measured with a ^7Li magnetic resonance fluxmeter, calibrated with the $^{13}\text{C}(\alpha, n)^{16}\text{O}$ resonance at $2.800 \pm \pm 0.003 \text{ MeV}^7$.

Targets have been used of natural magnesium, and of enriched ^{24}Mg , both evaporated onto copper backings.

The γ radiation produced was detected with a NaI scintillation crystal, 10 cm long and 10 cm in diameter.

In fig. 2 a yield curve is shown for α -particle energies between 1.2 and 3.2 MeV. With a differential discriminator γ -ray energies were selected in a $E_\gamma \approx 8\text{--}13 \text{ MeV}$ channel. Three different targets were used for different parts of the yield curve, as indicated in the figure caption.

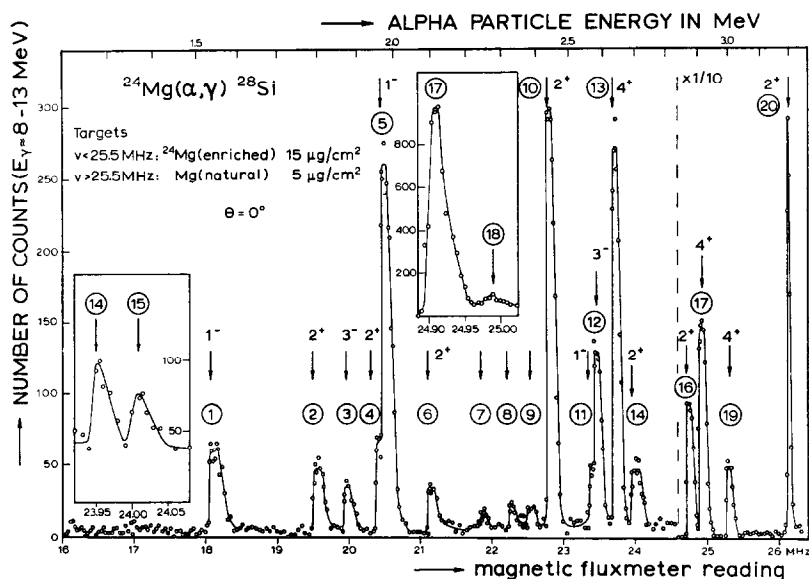


Fig. 2. Yield curve of the $^{24}\text{Mg}(\alpha, \gamma)^{28}\text{Si}$ reaction in the $E_\alpha = 1.2\text{--}3.2 \text{ MeV}$ region. High-energy γ radiation ($E_\gamma \approx 8\text{--}13 \text{ MeV}$) is detected with a NaI scintillation crystal (10 cm long and 10 cm in diameter), as close to the target as possible at 0° to the beam. For $E_\alpha < 3.1 \text{ MeV}$ an enriched ^{24}Mg target was used of $15 \mu\text{g}/\text{cm}^2$; for $E_\alpha > 3.1 \text{ MeV}$ the target was natural Mg of $5 \mu\text{g}/\text{cm}^2$ thickness; the parts of the yield curve shown in the two inserts were taken with a natural Mg target of about $3 \mu\text{g}/\text{cm}^2$ thickness.

At all resonances shown in fig. 2 (resonance 18 excepted) γ -ray spectra have been taken with a 400-channel pulse analyser, showing that these resonances have to be ascribed to the $^{24}\text{Mg}(\alpha, \gamma)^{28}\text{Si}$ reaction. The arguments for the assignment of resonance 18 to this reaction are given in section 8. The spectra are discussed in section 4.

The region below $E_\alpha = 3.1 \text{ MeV}$ has also been covered with a natural Mg

target which, however, did not show any new resonances. This is understandable because α -particle capture in ^{25}Mg and ^{26}Mg leads to neutron-unstable compound states in ^{29}Si and ^{30}Si , respectively.

Yield curves have also been taken with a γ -ray channel covering the $E_\gamma = 3\text{--}8\text{ MeV}$ region. The strong background observed in this channel closely follows the published¹⁾ yield curve of the $^{13}\text{C}(\alpha, n)^{16}\text{O}$ reaction, which shows pronounced resonances. The neutrons, presumably produced in carbon deposits on the magnet chamber walls, on slits, and on the target, contribute to the background by capture in the scintillation crystal. The carbon deposit on the target was kept to a minimum by passing the beam through a liquid air trap between the magnet and the target. The performance of this trap was very satisfactory as no rise in background or shift in resonance energies could be detected after several hours of bombardment.

The observed resonance energies are given in table II, column 2. The corresponding ^{28}Si excitation energies are given in table II, column 3. They

TABLE II

Resonances in the $^{24}\text{Mg}(\alpha, \gamma)^{28}\text{Si}$ reaction.					
1	2	3	4	5	6
Resonance number	E_α (MeV \pm keV)	$E_x(^{28}\text{Si})$ (MeV)	Main γ transitions (MeV)	$\frac{\Gamma_{\gamma 0}}{\Gamma_{\gamma 1}}$	$(2J + 1) \times \frac{\Gamma_\alpha \Gamma_\gamma}{\Gamma_g}$ (eV)
1	1.529 ± 5	11.296	γ_0, γ_1 ; 1.77 ^{a)}	2.5	0.11
2	1.785 ± 6	11.516	γ_1 ;	< 0.05	0.065
3	1.865 ± 6	11.584	γ_1 ; 1.77	< 0.05	0.05
4	1.950 ± 6	11.657	γ_0, γ_1 ; 7.85, (4.8), (3.7), 1.77	0.5	0.075
5	1.964 ± 6	11.670	γ_0, γ_1 ; 1.77 ^{b)}	0.06	0.30
6	2.093 ± 6	11.780	γ_1 ;	< 0.05	0.045
7	2.234 ± 7	11.901	γ_2 ;		0.025
8	2.323 ± 6	11.977	γ_2 ; 6.9, 5.1		0.05
9	2.378 ± 6	12.024	6.9, 5.1 ^{c)} ;		0.035
10	2.435 ± 5	12.073	γ_0, γ_1 ; 5.15, 4.5	6	0.40
11	2.566 ± 5	12.185	$\gamma_0, 10.9, \gamma_1$; 1.77, 1.28 ± 0.02 ^{d)}	3	0.07
12	2.580 ± 5	12.197	γ_1 ; (7.6)	< 0.10	0.18
13	2.634 ± 5	12.243	γ_1 ; see also fig. 13	< 0.05	0.38
14	2.692 ± 5	12.293	γ_1 ;	< 0.15	0.05
15	2.704 ± 5	12.304	γ_1 ;	< 0.20	0.035
16	2.869 ± 5	12.445	γ_0, γ_1 ; (7.5) ^{a)}	10	1.25
17	2.909 ± 5	12.479	γ_1 ; ^{e)}	< 0.07	2.0
18	2.926 ± 5	12.494	^{f)}		0.10
19	2.998 ± 5	12.556	γ_1 ; 7.5, 5.6, 5.1, 4.65, 2.84, 2.01	< 0.05	0.68
20	3.204 ± 6	12.732	γ_0, γ_1 ^{a)} ;	3.0	5.7

^{a)} $\Gamma_{\gamma 0} + \Gamma_{\gamma 1} < 0.85 \Gamma_\gamma$.
^{b)} $\Gamma_{\gamma 1} > 0.8 \Gamma_\gamma$.
^{c)} The two lines are of equal intensity.
^{d)} The 10.9 and 1.28 MeV transitions are in coincidence.
The intensity ratio of $\gamma_0, \gamma_{10.9}$ and γ_1 is 2 : 1 : 0.7.
^{e)} $\Gamma_{\gamma 1} > 0.9 \Gamma_\gamma$.
^{f)} No spectrum has been taken at this weak resonance.

were computed using a $^{24}\text{Mg}(\alpha, \gamma)^{28}\text{Si}$ Q value of 9.986 ± 0.003 MeV⁸). A discussion of these energies is given in section 7.

4. *Gamma-ray spectra.* The main characteristics of the observed γ -ray spectra are indicated in table II, column 4 and 5. Except at resonances 11 and 13 no coincidence spectra have been measured, which makes the interpretation of some of the observed lines a little doubtful. The 1.77 MeV line, e.g., is present at most resonances, but it is also prominent in the background at higher E_α , assumedly resulting from the $^{25}\text{Mg}(\alpha, n\gamma)^{28}\text{Si}$ reaction.

Resonance 4. The 3.7 and 7.85 MeV lines might form a cascade through the 7.93 MeV level. The 4.8 MeV line might feed the 6.88–6.89 MeV doublet.

Resonance 9. The equal intensity of the 6.9 and 5.1 MeV lines proves that these lines form a cascade through that component of the 6.88–6.89 MeV doublet, which mainly decays by a ground-state transition.

7	8	9	10	11	12
J^π	Quadrupole/dipole amplitude mixing ratio for γ_1	$^{27}\text{Al}(p, \gamma)^{28}\text{Si}$			$E_x(\alpha, \gamma) -$ $-E_x(p, \gamma)$ (keV)
		E_p (keV)	$E_x(^{28}\text{Si})$ (MeV)	J^π	
1 ⁻					
2 ⁺	-3.0 ± 0.5				
3 ⁻	$+0.02 \pm 0.02$				
2 ⁺					
1 ⁻	-0.09 ± 0.04				
2 ⁺	-0.10 ± 0.10	202.3 ± 0.9 ⁿ⁾	11.776		4
		326.0 ± 0.4 ^{h)}	11.895	4(-) ^{l)}	6
		404.9 ± 0.4 ^{h)}	11.971	4- ⁱ⁾	6
2 ⁺		504.8 ± 0.3 ^{h)}	12.067	2+ ^{k)} ⁱ⁾	6
1 ⁻					
3 ⁻	$+0.03 \pm 0.03$	632.1 ± 0.5 ⁿ⁾	12.190	3- ^{k)}	7
4 ⁺		679.2 ± 0.5 ⁿ⁾ ^{m)}	12.236 ^{m)}	3+ ^{k)} ^{m)}	7 ^{m)}
2 ⁺	$+0.60 \pm 0.05$	731.2 ± 0.5 ⁿ⁾	12.286	2+ ^{k)}	7
		742.1 ± 0.7 ^{h)}	12.296	2+ ^{k)}	8
2 ⁺		885 ± 2 ^{h)}	12.434		11
4 ⁺		923.1 ± 0.3 ^{h)}	12.471		8
		937.6 ± 0.3 ^{h)}	12.485	3- ^{l)}	9
4 ⁺		1002.5 ± 0.5 ^{h)}	12.547		9
2 ⁺		1183.4 ± 0.4 ^{h)}	12.722	2+ ^{l)}	10

^{g)} Only those lines are included in Γ_γ which are indicated in column 4 to the left of the semicolon.

^{h)} Averages of measurements by several authors (see text).

ⁱ⁾ Ref. 15.

^{j)} Ref. 16.

^{k)} Ref. 17.

^{l)} These two J^π determinations are from $^{27}\text{Al}(p, \alpha)^{24}\text{Mg}$ ¹⁸⁾.

^{m)} This resonance does *not* correspond to the (α, γ) resonance 13, see text.

ⁿ⁾ Present work.

Resonances 6, 7, 8, 10, 12, 14, and 15. It will be shown in section 7 that these resonances very probably correspond to known $^{27}\text{Al}(p, \gamma)^{28}\text{Si}$ resonances. The main features of the (α, γ) decay agree well with those found in much more detail from the (p, γ) work.

Resonances 13 and 18. These resonances will be discussed in more detail in sections 7 and 8, respectively. The γ spectrum at resonance 13 is shown in fig. 3.

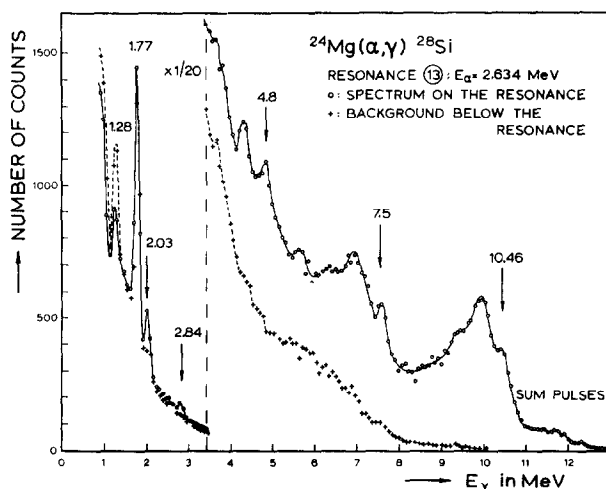


Fig. 3. Gamma spectrum at resonance 13 ($E_\alpha = 2.63 \text{ MeV}$). The dashed curve represents the background, measured just below the resonance.

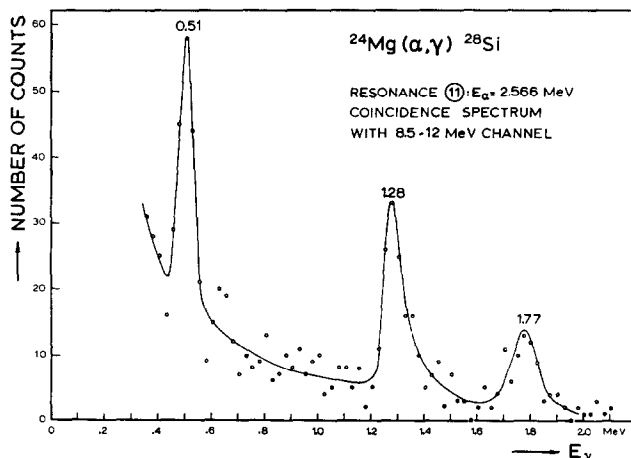


Fig. 4. Gamma spectrum at resonance 11, in coincidence with the radiation in a $E_\gamma = 8.5\text{--}12.0 \text{ MeV}$ channel.

Resonance 11. At the higher E_α the 1.28 MeV line is also prominent in the background, probably resulting from the $^{19}\text{F}(\alpha, p)^{22}\text{Ne}$ reaction, leading to $^{22}\text{Ne}(1)$ at $1.274 \pm 0.002 \text{ MeV}$, or from $^{26}\text{Mg}(\alpha, n)^{29}\text{Si}$, leading

to the ^{29}Si first excited state at 1.277 ± 0.004 MeV⁹). The appearance of the 10.9 MeV line, however, in coincidence with the 1.28 MeV line, requires these lines to be interpreted as a cascade through a new 10.90 ± 0.02 MeV level in ^{28}Si . The γ spectrum, in coincidence with the radiation in a 8.5–12.0 MeV channel, is shown in fig. 4. In an analogous coincidence run taken just below the resonance, the 1.28 and 1.77 MeV lines are completely absent.

Resonance 19. An interpretation of most of the observed lines is hazardous without measurements of coincidence spectra.

5. *Absolute yields.* Thick target yield measurements have been performed from which the resonance strengths $(2J + 1) \Gamma_\alpha \Gamma_\gamma / \Gamma$ can be found¹⁰), taking into account the target stopping power¹¹), and the counter solid angle and efficiency. Corrections for angular distribution have been applied, if known (see section 6). The resulting resonance strengths are given in table II, column 6. The errors might amount to 30% at the strong resonances, and up to a factor of two at the weakest resonances.

In the yield measurements only those lines have been taken into account which are indicated in table II, column 4, to the left of the semicolon. The "partial yields" thus found might be somewhat smaller than the total yields, in which all transitions deexciting the resonance level are included, by an amount differing from resonance to resonance.

6. *Angular distributions and correlations.* In comparing the theoretical expressions for angular distributions and correlations with experiment, solid angle attenuation factors have to be applied. In the case of angular distributions, the theoretical A_2 and A_4 coefficients have to be multiplied with the attenuation factors Q_2 and Q_4 , respectively. For angular correlations the same values of Q_2 and Q_4 can be used, but they enter in a more complicated way (see e.g. ref. 12). All measurements were made with two scintillation crystals, both 10 cm long and 10 cm in diameter, with, generally, the surface of the crystals at a distance $D = 10$ cm from the target. In this case the attenuation factors as computed through an approximation given by Hoogenboom¹²) are $Q_2 = 0.93$ and $Q_4 = 0.76$. These values are in good agreement with measurements of the attenuation factors, to be described at the end of this section. Analogous measurements (see below) give the attenuation factors $Q_2 = 0.83$, $Q_4 = 0.47$, for a counter distance $D = 5$ cm, which has been used at some of the weaker resonances.

Discriminator channels were set with the aid of the pulse-height analyser using a self-gating procedure. Care was taken to ensure that contributions from unwanted γ transitions or cascades were negligible.

Background, as measured just below the resonances, has been subtracted. For the angular correlation measurements, with a coincidence resolving time of 1 μsec , the background was negligible.

Any excentricity of the target spot with respect to the center of the counter turntable was measured and corrected for by calibrating on the isotropic 622 keV $^{30}\text{Si}(p, \gamma)^{31}\text{P}$ resonance.

Results are presented in figs. 5 to 10. Drawn curves correspond to the theoretical expressions, computed as indicated in section 2 with solid angle attenuation taken into account.

The angular distributions of γ_0 have been measured at the six resonances 1, 4, 10, 11, 16, and 20 (fig. 5).

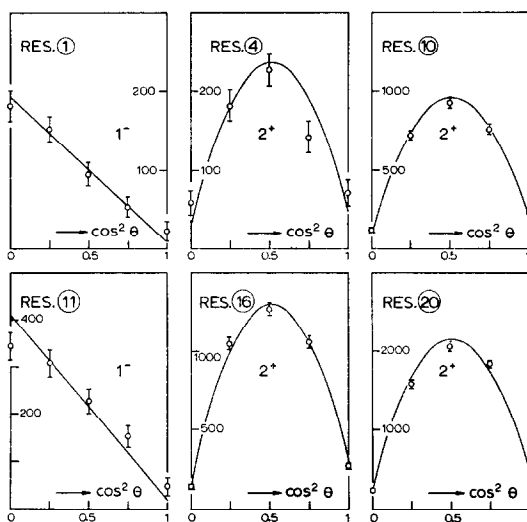


Fig. 5. Measured angular distributions of γ_0 at resonances 1, 4, 10, 11, 16, and 20. The curves correspond to the theoretical expressions given in fig. 2a, normalized to the measured total number of counts. Background has been subtracted. Distance between target and front of crystal $D = 10$ cm.

Although statistics are poor in some cases, it is seen that a unique decision as to the J^π of these resonances (either 1^- or 2^+) can be made.

Next, resonances 13, 17, and 19 will be considered (fig. 6). The γ_1 angular distribution measurements yield the alternatives $J^\pi = 4^+$, or $J^\pi = 2^+$ with an $M1-E2$ amplitude mixing ratio $x \approx -2$. The angular correlation of γ_1 and the $E_\gamma = 1.77$ MeV γ ray measured in geometry II excludes the latter possibility and decides in favour of $J^\pi = 4^+$.

At resonances 3 and 12 (fig. 7) the γ_1 angular distribution would be in agreement with a pure or almost pure $E1$ $3^- \rightarrow 2^+$ transition, with a mixed $M1 + E2$ $2^+ \rightarrow 2^+$ transition with $x \approx 0.7$, or with a mixed $E1 + M2$ $1^- \rightarrow 2^+$ transition with $x \approx -0.2$. The angular correlation in geometry II agrees well with $J^\pi = 3^-$, and excludes $J^\pi = 2^+$ and 1^- , although some doubt might remain as to the possibility of the latter.

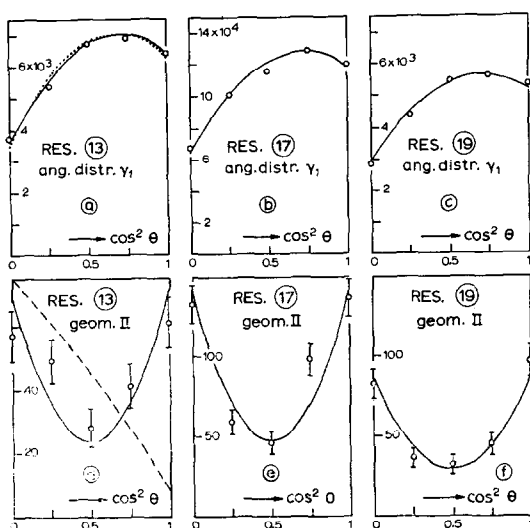


Fig. 6. Measured angular distributions of γ_1 (a, b and c), and angular correlations (d, e, and f) of the cascade through $^{28}\text{Si}(1)$ in geometry II, at resonances 13, 17, and 19. Solid curves correspond to the theoretical expressions for $J^\pi = 4^+$; dashed curves correspond to $J^\pi = 2^+$ with $\alpha = -2.3$ for γ_1 . Normalization as in fig. 5. Background subtracted. For a, b, and c, $D = 10$ cm; for d, e, and f, $D = 10$ cm for both crystals.

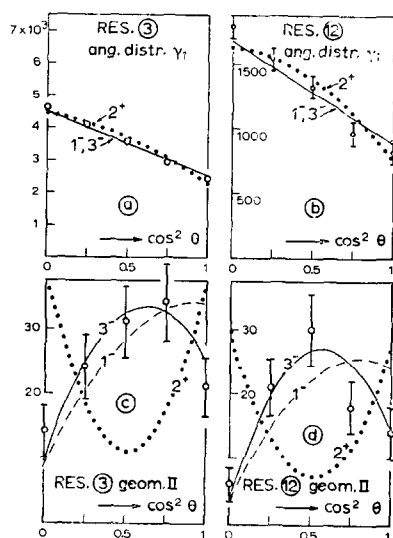


Fig. 7. Measured angular distributions of γ_1 (a and b), and angular correlations (c and d) of the cascade through $^{28}\text{Si}(1)$ in geometry II, at resonances 3 and 12. Solid curves correspond to the theoretical expressions for $J^\pi = 3^-$ and $\alpha = 0$ for γ_1 ; dotted curves correspond to $J^\pi = 2^+$ with $\alpha = +0.7$; the dashed curves correspond to $J^\pi = 1^-$ with $\alpha = -0.22$. The $J^\pi = 1^-$, $\alpha = -0.22$, γ_1 angular distribution coincides with that for $J^\pi = 3^-$, $\alpha = 0$. Normalization as in fig. 5. Background subtracted. For a, $D = 5$ cm; for b, $D = 10$ cm; for c, $D = 5$ cm for the rotating counter and 10 cm for the fixed counter; for d, $D = 10$ cm for both counters.

The γ_1 angular distribution at resonance 2 (fig. 8) fits best with a $2^+ \rightarrow 2^+$ transition, with a $M1-E2$ mixing ratio of $\alpha = 3.0 \pm 0.5$, although a pure $E2$ $4^+ \rightarrow 2^+$ transition is not quite impossible. The angular correlation in geometry VI excludes $J^\pi = 4^+$.

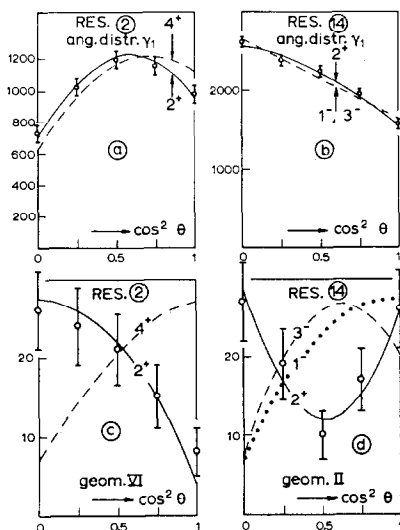


Fig. 8. Measured angular distributions of γ_1 (a and b), and angular correlations (c and d) of the cascade through $^{28}\text{Si}(1)$ in geometries VI and II, at resonances 2 and 14, respectively. At resonance 2 the solid curves correspond to $J^\pi = 2^+$ and $\alpha = 3.0$ for γ_1 ; dashed curves correspond to $J^\pi = 4^+$, $\alpha = 0$. At resonance 14, solid curves correspond to $J^\pi = 2^+$, $\alpha = 0.60$; dashed or dotted curves to $J^\pi = 3^-$, $\alpha = -0.03$ and $J^\pi = 1^-$, $\alpha = -0.17$. Normalization as in fig. 5. Background subtracted. For a, $D = 10$ cm, for b, $D = 5$ cm, for c, $D = 5$ cm for the fixed counter and 10 cm for the rotating counter, for d, $D = 10$ cm for the fixed counter and 5 cm for the rotating counter.

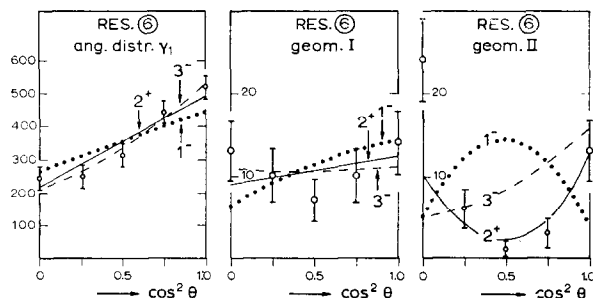


Fig. 9. Measured angular distribution of γ_1 (a), and angular correlations of the cascade through $^{28}\text{Si}(1)$ in geometries I and II (b and c), at resonance 6. Solid curves correspond to the theoretical expressions for $J^\pi = 2^+$, $\alpha = -0.10$, dashed curves to $J^\pi = 3^-$, $\alpha = -0.50$, dotted curves to $J^\pi = 1^-$, $\alpha = 0.75$. Normalization from least-squares analysis. Background subtracted. For a, $D = 10$ cm, for b and c, $D = 5$ cm for the fixed counter and 10 cm for the rotating counter.

The γ_1 angular distribution at resonance 14 (fig. 8) could be explained as an almost pure $E1\ 3^- \rightarrow 2^+$ transition, as a $1^- \rightarrow 2^+$ transition with $x \approx -0.2$, or as a $2^+ \rightarrow 2^+$ transition with $x = +0.60 \pm 0.05$. The angular correlation in geometry II decides in favour of the latter case.

The angular distribution of γ_1 at resonance 6 (fig. 9) agrees with $J^\pi = 2^+$ ($x = -0.10 \pm 0.10$), with $J^\pi = 3^-$ ($x = -0.50$), and perhaps also with $J^\pi = 1^-$ ($x = 0.75$). The angular correlation of the cascade through $^{28}\text{Si}(1)$ in geometry II decides in favour of the $J^\pi = 2^+$ assignment.

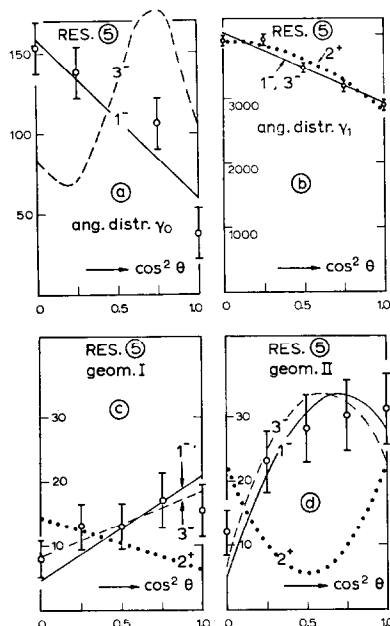


Fig. 10. Measured angular distributions of γ_0 (a) and γ_1 (b), and angular correlations (c and d) of the cascade through $^{28}\text{Si}(1)$ in geometries I and II, at resonance 5. In b, c and d, solid curves correspond to $J^\pi = 1^-$, $x = -0.09$, dotted curves to $J^\pi = 2^+$, $x = 0.47$, dashed curves to $J^\pi = 3^-$, $x = -0.08$. Normalization from least-squares analysis. Background in figs. 10a and b and also contribution of γ_0 in fig. 10b subtracted. Sum pulses of $9.99 + 1.77$ MeV γ rays, of which the angular distribution was computed, contribute to the angular distribution of γ_0 with an assumed intensity of 33% of γ_0 . For a and b, $D = 10$ cm, for c and d, $D = 5$ cm for the fixed counter and 10 cm for the rotating counter.

The angular distribution of γ_1 at resonance 5 would agree with $J^\pi = 1^-$ ($x = -0.09 \pm 0.04$), $J^\pi = 2^+$ ($x = 0.47$) or $J^\pi = 3^-$ ($x = -0.08$) (fig. 10). The angular correlations of the cascade through $^{28}\text{Si}(1)$ measured in geometries I and II clearly exclude $J^\pi = 2^+$. The angular distribution of the weak ground state transition has also been measured. Because of the relative weakness of γ_0 , sum pulses of the cascade through $^{28}\text{Si}(1)$ will contribute to the measured distribution. The curves drawn in fig. 10a give the theoretical

curves for the $J^\pi = 1^-$ and 3^- cases on the assumption that the sum-pulse intensity is one third of that of γ_0 . The sum-pulse angular distributions, which may be considered as angular correlations where both γ 's are detected in the same counter have been computed using the Ferguson and Rudledge tables⁶⁾. Apparently, only $J^\pi = 1^-$ agrees with the measurements. Of course the fact that a γ_0 is observed, already makes a $J^\pi = 3^-$ assignment quite improbable.

The J^π values and mixing ratios obtained above are given in table II, column 7 and 8, respectively.

The pronounced γ_0 angular distributions, in which no mixing parameters have to be fitted, offer an ideal opportunity for direct measurement of the solid angle attenuation factors Q_2 and Q_4 . Least squares fits of the angular distributions at the strong 2^+ resonances 10, 16, and 20 measured with a $D = 10$ cm counter distance yielded $Q_2 = 0.92, 0.91$, and 0.96 , all ± 0.03 , and $Q_4 = 0.71, 0.76$, and 0.73 , all ± 0.02 respectively. The averages $Q_2 = 0.93 \pm 0.02$, $Q_4 = 0.73 \pm 0.02$, are in reasonable agreement with the theoretically computed values $Q_2 = 0.93$, $Q_4 = 0.76$, which had been used to correct all the $D = 10$ cm measurements. A measurement at resonance 16 yielded the $D = 5$ cm attenuation factors $Q_2 = 0.83 \pm 0.03$, $Q_4 = 0.47 \pm 0.02$.

7. *Comparison with $^{27}\text{Al}(\beta, \gamma)^{28}\text{Si}$ and $^{27}\text{Al}(\beta, \alpha)^{24}\text{Mg}$ results.* A. Excitation energies. Most (α, γ) resonances above $E_\alpha = 2.2$ MeV correspond to known $^{27}\text{Al}(\beta, \gamma)^{28}\text{Si}$ resonances and many also correspond to known $^{27}\text{Al}(\beta, \alpha)^{24}\text{Mg}$ resonances. Several precision measurements exist of the (β, γ) resonance energies^{13) 14) 15) 16)}.

In view of the importance of determining the exact position of the 679 keV resonance (see section 7B) the energies of the 632, 679 and 731 keV $^{27}\text{Al}(\beta, \gamma)^{28}\text{Si}$ resonances were remeasured, yielding 632.1, 679.2 and 731.2 keV respectively, all ± 0.5 keV. The error in the energy differences is estimated as 0.2 keV. If one takes into account the recent change in the energy of the $^{27}\text{Al}(\beta, \gamma)^{28}\text{Si}$ resonance, used as a calibration, from 990.8 keV to 992.0 ± 0.5 keV¹⁷⁾, these values check well with those given in ref. 14 but not very well with those of ref. 15. The energy differences between the (α, γ) resonances 12, 13, and 14 have also been measured with better precision than is evident from table II, column 2. The final ^{28}Si excitation energy corresponding to resonance 13, as measured relative to resonances 12 and 14, agrees within the experimental error with that corresponding to the 679 keV (β, γ) resonance, the (α, γ) excitation energy actually being 0.6 ± 0.6 keV higher.

The other values given in table II, column 9, are averages of measurements by several authors. These values have been corrected for the change in the calibration mentioned above. With a Q value of 11.5806 ± 0.0033 MeV⁶⁾,

the corresponding ^{28}Si excitation energies have been computed, as given in table II, column 10.

When the weak (α, γ) resonances 6, 9, and 11 were found, it was thought interesting to search for the corresponding (p, γ) resonances which were not known at the time, and which could be expected at $E_p = 201, 453,$ and 620 keV, respectively. This has been done with the Utrecht 900 kV cascade generator. As a result, a new, extremely weak, $^{27}\text{Al}(p, \gamma)^{28}\text{Si}$ resonance has been found at $E_p = 202.3 \pm 0.9$ keV. The yield is about one fifth of the known $E_p = 224$ keV resonance. A yield curve showing the 202 and 224 keV resonances is given in fig. 11. The γ spectrum at the new resonance shows 10.0 and 1.77 MeV transitions which agrees with the spectrum at the corresponding (α, γ) resonance 6. The (p, γ) resonances corresponding to the (α, γ) resonances 9 and 11 have not been detected.

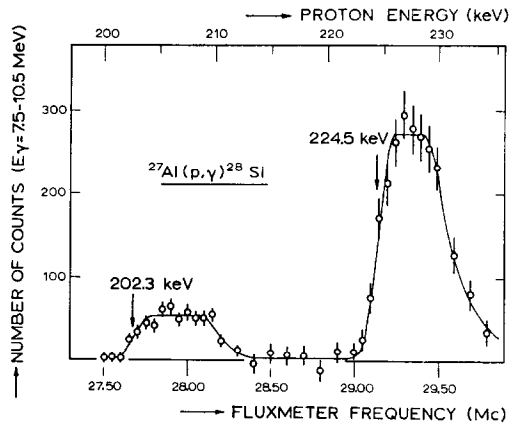


Fig. 11. Low energy yield curve of the $^{27}\text{Al}(p, \gamma)^{28}\text{Si}$ reaction showing the new $E_p = 202.3 \pm 0.9$ keV resonance. Machine-off background has been subtracted.

The correspondence between the ^{28}Si excitation energies as found from the (α, γ) and (p, γ) reactions is seen to be good, although systematically the values from the (α, γ) work are somewhat higher, by an amount increasing from 4 to 10 keV (table II, column 12).

Part of the observed energy differences might be explained by saturation of the deflecting magnet distorting the proportionality between the average field on the particle orbit and the field at the position of the resonance fluxmeter coil. This effect would account for the increase with energy of the energy differences in column 12. The existence of magnet saturation has also been demonstrated by the observation of a small difference in the fluxmeter calibration constants obtained from the 992.0 keV $^{27}\text{Al}(p, \gamma)^{28}\text{Si}$ resonance and the 2800 keV $^{13}\text{C}(\alpha, n)^{16}\text{O}$ resonance. Calibration with the former resonance would increase all α -particle energies with 0.28%, yielding energy differences in column 12 from 9 to 17 keV.

The fact that the values in column 12 do not go through zero at $E_\alpha = 2800$ keV, implies that there might also be errors in the energy of the $^{13}\text{C}(\alpha, n)^{16}\text{O}$ resonance used for the calibration and/or in the assumed value of the $^{27}\text{Al}-^{24}\text{Mg}$ mass difference. A recent precision measurement of the $^{27}\text{Al}(p, \alpha)^{24}\text{Mg}$ and $^{24}\text{Mg}(\alpha, p)^{27}\text{Al}$ Q values would effect a decrease of 3.5 keV in the values in column 12¹⁸⁾.

If target surface layers (see section 3) would have been responsible for the observed discrepancies, the values in column 12 should have decreased with increasing particle energy.

The errors assigned to the (α, γ) resonance energies in table II, column 2, are compounded from;

- a) the contribution, proportional to E_α , resulting from the error in the calibration energy;
- b) the error, also taken proportional to E_α , in the determination of the low-energy edge of a resonance peak;
- c) the estimated error due to magnet saturation.

B. Spins and parities. The J^π values of $^{27}\text{Al}(p, \gamma)^{28}\text{Si}$ resonances, below $E_p = 750$ keV, as determined from angular distribution and correlation measurements^{19) 20) 21)}, are listed in table II, column 11. Spins and parities of levels 18 and 20 have been determined from $^{27}\text{Al}(p, \alpha)^{24}\text{Mg}$ angular distribution measurements²²⁾.

It is seen that the J^π values given in column 7 and 11 of table II agree at resonances 10, 12, 14, and 20.

Resonances 7 and 8 should have $J^\pi = 4^+$ rather than $J^\pi = 4^-$. The odd parity assignment was mainly based on the fact that no measurable $^{27}\text{Al}(p, \alpha)^{24}\text{Mg}$ yield had been observed at these resonances, which, apparently, is an unreliable criterion.

Resonance 13, finally, deserves a special discussion. For some time it was thought that this resonance would correspond to the 679 keV $^{27}\text{Al}(p, \gamma)^{28}\text{Si}$ resonance, because the ^{28}Si excitation energies as measured relative to neighbouring resonances check within the experimental error (see section 7A). The main features of the γ -ray spectra (see fig. 3 and ref. 2) also agree. In a yield measurement with a very thin target (0.5 keV total energy resolution) no sign has been found of the 679 keV (p, γ) resonance being double. The present (α, γ) work, however, yields a unique 4^+ assignment, while the (p, γ) angular correlation measurements²¹⁾ can by no means be explained with a 4^+ resonant level, not even if the possibility of $E2-M3$ mixing is considered; they yield a unique 3^+ assignment. The only conclusion can be that different ^{28}Si levels are excited through the (α, γ) and (p, γ) reactions.

This conclusion has been confirmed by a comparison of (α, γ) and (p, γ) coincidence spectra. Gamma-gamma coincidence spectra have been measured at the (α, γ) resonance 13 with 8.2–11.0, 5.5–8.0, 4.0–5.1, and 3.1–3.9 MeV

channels, using two 10×10 cm NaI crystals as close to the target as possible. Coincidence spectra at the 679 keV (p, γ) resonance are already given in ref. 2, but for comparison the spectra with 8.2–11.0 and 5.5–8.0 MeV channels were remeasured using the Van de Graaff H_2^+ beam. Several differences are evident in the (α, γ) and (p, γ) spectra with corresponding channels.

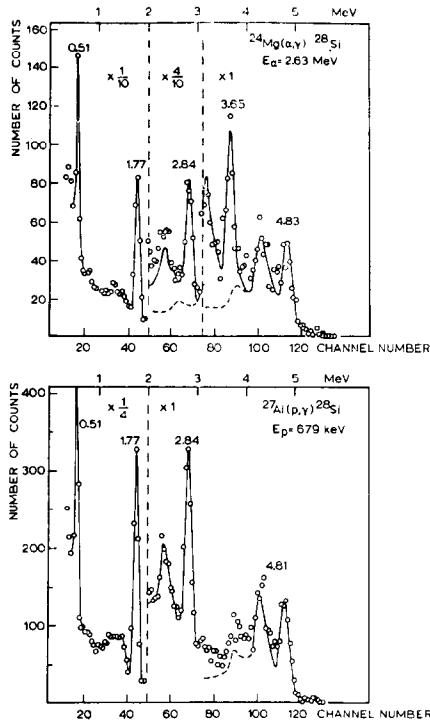


Fig. 12. Gamma-gamma coincidence spectra with a $E_\gamma = 5.5$ –8.0 MeV channel, taken at the $E_\alpha = 2.63$ MeV $^{24}\text{Mg}(\alpha, \gamma)^{28}\text{Si}$ resonance (resonance 13), and at the $E_p = 679$ keV $^{27}\text{Al}(p, \gamma)^{28}\text{Si}$ resonance. The occurrence of the 3.65 MeV γ ray in the (α, γ) work shows that these resonances decay differently.

The main difference is the appearance of the (α, γ) 3.65 MeV transition to the 8.59 MeV level which is absent at the (p, γ) resonance (see fig. 12). The spectra in fig. 12 were taken on the same day with the same scintillation counters. In the second place the (α, γ) resonance shows a transition to the 7.37 MeV level, decaying with about equal intensities to $^{28}\text{Si}(0)$ and $^{28}\text{Si}(1)$ while the (p, γ) resonance shows a transition to the 7.42 MeV level, almost completely decaying to $^{28}\text{Si}(0)$. The corresponding decay schemes are given in fig. 13.

In the (p, γ) work it was shown²⁾ that the 2.84 MeV transition has to be regarded as a primary feeding a 9.39 MeV level. In the (α, γ) work it could not be decided if the 2.84 MeV γ ray is a primary or a secondary. In fig. 13a

it has been shown in the most probable position, connecting $^{28}\text{Si}(2)$ to $^{28}\text{Si}(1)$.

The 7.37 MeV level, at the (α, γ) resonance, is excited from a 4^+ state, and deexcited to the 0^+ ground state. The 7.37 MeV level then very probably has $J^\pi = 2^+$, because any other assumption would necessitate the occurrence of $M2$ or octupole transitions.

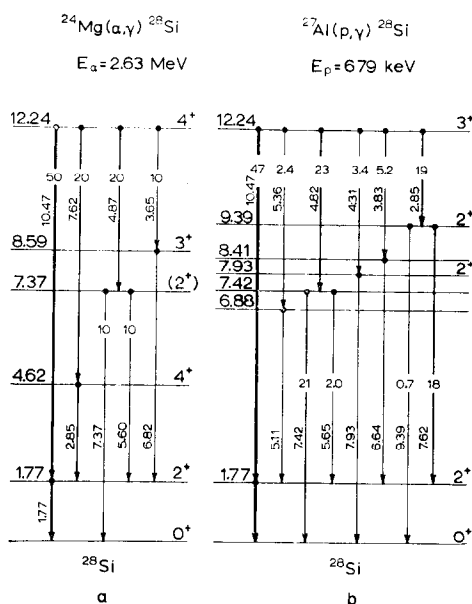


Fig. 13. Decay schemes of the two ^{28}Si levels at $E_x = 12.24$ MeV, one excited through the $^{24}\text{Mg}(\alpha, \gamma)^{28}\text{Si}$ reaction, the other (as taken from ref. 2) through the $^{27}\text{Al}(p, \gamma)^{28}\text{Si}$ reaction. In the (α, γ) work the order of the 7.62 and 2.84 MeV γ rays is not certain; they could also form a cascade through a 9.4 MeV level.

C. Radiation mixing ratios. Only at resonance 14, the $M1 - E2$ amplitude mixing ratio as found from the (α, γ) work, can be compared with that found from (p, γ) angular correlation measurements. The results $\alpha = +0.60 \pm 0.05$ (Table II, column 8) and $\alpha = +0.49 \pm 0.08^{21}$, respectively, agree within the experimental error.

8. *Partial widths.* From measurements of the strengths of corresponding resonances in the $^{24}\text{Mg}(\alpha, \gamma)^{28}\text{Si}$, $^{27}\text{Al}(p, \gamma)^{28}\text{Si}$, and $^{27}\text{Al}(p, \alpha)^{24}\text{Mg}$ reactions it is possible to deduce the relevant partial widths, Γ_α , Γ_p , and Γ_γ . In some cases the total width Γ has also directly been measured, yielding a check on the results obtained.

The data are given in table III. The (α, γ) yields in column 3 are taken from table II; at resonances 7, 8, 10, 12, 14, and 15, where the γ decay is well known from the (p, γ) work, and also at resonance 13 where the decay scheme was investigated in the present work, the "partial" yields have first

TABLE III
Partial widths of ^{28}Si resonant states.

1	2	3	4	5	6	7	8	9	10
Resonance number	J^π a)	$(2J+1) \times \Gamma_\alpha \Gamma_\gamma / \Gamma^b$ (eV)	$(2J+1) \times \Gamma_p \Gamma_\gamma / \Gamma^c$ (eV)	$(2J+1) \times \Gamma_p \Gamma_\alpha / \Gamma^c$ (eV)	Γ^e (eV)	Γ_α^d (eV)	Γ_p^d (eV)	Γ_γ (eV)	$\mathcal{B}_{\alpha^2 d} \times 10^3$
1	1-	0.11				(0.037)			(85)
2	2+	0.065				(0.013)			(5)
3	3-	0.05				(0.007)			(7)
4	2+	0.075				(0.015)			(1.5)
5	1-	0.30				(0.10)			(4)
6	2+	0.045	0.00017			(0.009)	(3×10^{-8})		(0.4)
7	(4+)	0.035	0.028			(0.004)	(0.003)		(1.3)
8	(4+)	0.07	0.15			(0.008)	(0.017)		(1.4)
9		0.035	< 0.004						
10	2+	0.50	0.95	1.5	< 200	0.6	1.1	0.35	2.3
11	1-	0.07	< 0.002						
12	3-	0.23	5.4			0.8	18	0.8	5.1
13	4+	0.75		5.0	< 60				
14	2+	0.09	4.0	< 0.4	< 1000	1.2	54	0.8	1.3
15	2-	0.075	0.4	5.9	< 160				
16	2+	1.25	1.0	< 0.4	< 1000	4.8	3.8	0.48	2.4
17	4+	2.0	4.3	10	< 190	0.9	1.9	0.9	7.0
18	3-	0.10	4	65	340 ± 110	9.5	380	0.6	14
19	4+	0.68	1.0	2.4	< 1000	0.5	0.8	0.22	2.4
20	2+	5.7	4.7	940	710 ± 130	420	340	2.1	65

a) Combined results from (α, γ) , (p, γ) , and (p, α) measurements.
 b) From table II, column 6, after converting "partial" yields into total yields (see text).
 c) From ref. 9, except for resonances 6, 9, and 11 (present work).
 d) The values put in brackets were computed making the assumptions $\Gamma_\gamma \gg \Gamma_\alpha$ and $\Gamma_\gamma \gg \Gamma_p$.
 If the assumptions are not fulfilled the bracketed values can always be regarded as lower limits.

been converted into total yields (see also section 5). The (p, γ) and (p, α) yields and the total widths in column 4, 5, and 6, respectively, are given and discussed in ref. 9. It is believed at present that the (p, α) yields given in ref. 20 are systematically low. They were multiplied by a factor of 1.9 to get agreement with the yield at the 731 keV resonance given in ref. 22. The (p, γ) yield at resonance 6, and the upper limits on the (p, γ) yield at resonances 9 and 11, result from the $^{27}\text{Al}(p, \gamma)^{28}\text{Si}$ run mentioned in section 7A.

From columns 3, 4, and 5, the partial widths Γ_α , Γ_p , and Γ_γ can be found as listed in columns 7, 8, and 9, respectively. It has been assumed that only γ emission, and particle emission to the ^{27}Al and ^{24}Mg ground states contributes. At the very highest energies, transitions to $^{27}\text{Al}(1)$ and (2) , and to $^{24}\text{Mg}(1)$ would also be possible, energetically, but Coulomb penetration factors would be relatively small.

It is seen in table III, that the (α, γ) resonances 6 through 20 all have a corresponding (p, γ) resonance, but for resonances 9, 11 and 13. There are, however, many (p, γ) resonances, not indicated in table III, which have no corresponding (α, γ) resonance. All (p, α) resonances correspond to an (α, γ) and to a (p, γ) resonance.

Resonances 18 and 20 are the only cases in which the total width Γ has been measured directly¹⁵⁾. It is seen that Γ_α , Γ_p , and Γ_γ add up to Γ , well within the experimental errors. Historically, resonance 18 was rather special. In the first (α, γ) runs with relatively thick targets, it was missed because it is situated closely above the strong resonance 17. Its existence and yield, however, could be predicted from the known (p, γ) and (p, α) yields and total width. Finally, it was detected, with the predicted yield, in a run with a very thin target (fig. 2, insert).

Resonance 20, the lowest ^{28}Si level with an appreciable α -particle width has also been observed as a resonance in the $^{24}\text{Mg}(\alpha, p)^{27}\text{Al}$ reaction, and in the elastic scattering of α particles on $^{24}\text{Mg}^{31}$.

In table III, column 10, the reduced α -particle widths $\theta_\alpha^2 = \Gamma_\alpha(A_l^2 \lambda \mu R / \hbar^2)$ are given, computed from Γ_α in column 7. The penetration factors A_l^2 were taken from the tables in ref. 23, using an interaction radius $R = 1.45 (A^{1/3} + 4^{1/3}) \times 10^{-13}$ cm; μ is the reduced mass. Apparently, none of the reduced widths is exceptionally large.

A discussion of Γ_p and Γ_γ and of the corresponding reduced transition probabilities will be given in a separate paper, dealing with the $^{27}\text{Al}(p, \gamma)^{28}\text{Si}$ angular distribution and correlation measurements, quoted as ref. 21.

Two facts, however, which should be mentioned here, are, first, the apparent large strengths of the even parity resonances as compared to those of the odd parity resonances, and, second, the apparent preference for $E2$ rather than $M1$ emission at the even parity resonances. For example, the strong 2^+ resonances 10, 16, and 20 mainly decay through γ_0 emission,

which is pure $E2$. The strong 4^+ resonances 13, 17, and 19, mainly decay through γ_1 emission, which, again, has pure $E2$ character. The 2^+ resonances 2 and 14, not decaying by γ_0 emission, anyway show a strong $E2$ contribution in the mixed $M1-E2$ γ_1 transitions.

This relative slowness of $E1$ and $M1$ transitions, as compared to $E2$ transitions, is most naturally explained by assuming that isobaric spin in ^{28}Si is still a rather good quantum number, even at excitation energies in the 11–13 MeV region. Alpha-particle capture in ^{24}Mg leads to the formation of $T = 0$ states in ^{28}Si , for which the $E1$ decay to lower ^{28}Si $T = 0$ states is forbidden, while the $M1$ decay is slowed down by a factor of about 100³⁰⁾.

The occurrence of $E1-M2$ mixing, at resonance 5, again points to the fact that the corresponding $E1$ transition is probably slow.

9. *The ^{28}Si 11.30 MeV level.* Recently, several experiments have been performed showing that there is a $J = 1$ ^{28}Si level at about 11.3 MeV with an exceptionally large radiation width.

Discrete γ rays have been observed in the fluorescence radiation from silicon samples irradiated with betatron or linear accelerator bremsstrahlung. The energy of the most intensive component is given as 11.2 MeV²⁴⁾, 11.40 ± 0.06 MeV²⁵⁾, 11.2 ± 0.05 MeV²⁶⁾, and 11.3 MeV²⁷⁾. There is also a weaker component with an energy of 9.4 MeV²⁴⁾²⁶⁾, or 9.8 MeV²⁷⁾. Threshold determinations²⁵⁾²⁷⁾ show that the higher energy component corresponds to a level in ^{28}Si at about 11.3 MeV. The lower energy component might be the transition from an 11.3 MeV level to $^{28}\text{Si}(1)^{26)}$, although a corresponding break in the yield curve has also been observed²⁷⁾. Self-absorption measurements of the radiation width for γ_0 emission from the 11.3 MeV level are at variance, yielding 2.9 ± 0.9 eV²⁵⁾, 8.3 ± 2.5 eV²⁷⁾, and 115 ± 30 eV²⁶⁾. The γ_0/γ_1 intensity ratio has been given as 1.8²⁶⁾. The γ_0 angular distribution is consistent with dipole absorption²⁶⁾.

The same level has been seen by magnetic analysis of electrons, inelastically scattered on silicon, at $E_e = 40$ MeV²⁸⁾. A sharp peak was found at $E_x = 11.6$ MeV, and a broad one of comparable intensity at 20 MeV, the latter corresponding to the giant resonance. The radiation width is $1030 \pm \pm_{230}^{310}$ eV for $E1$ excitation or $47 \pm_{9}^{14}$ eV for $M1$ excitation. The ratio of the intensities at $\theta = 132^\circ$ and 167° favours $M1$ excitation.

Levels with analogous properties have been found in ^{12}C at 15.11 MeV ($J^\pi = 1^+, T = 1$) and in ^{24}Mg at about 10.5 MeV ($J = 1$).

It is very tempting to identify the 1^- level in ^{28}Si at $E_x = 11.296$ MeV found from the $^{24}\text{Mg}(\alpha, \gamma)^{28}\text{Si}$ reaction, with the 11.3 MeV $J = 1$ level found from the $^{28}\text{Si}(\gamma, \gamma)^{28}\text{Si}$ and $^{28}\text{Si}(e, e')^{28}\text{Si}$ reactions. The excitation energy, the spin, and the branching ratio are in good agreement. The parity, however, would appear from the (e, e') work to be even rather than odd.

Furthermore, it would seem difficult to understand why a level with a

relatively large α -particle reduced width, and thus of high $T = 0$ isobaric spin purity, would have a large dipole radiation width (see section 8).

One could consider a direct measurement of the radiation width in an (α, γ) resonance absorption experiment²⁹), but for this purpose resonance 1 is too weak.

10. *Conclusion.* The (α, γ) reaction, especially on even-even initial nuclei has proved a valuable tool in nuclear spectroscopy. Angular distribution measurements, supplemented, if necessary, with angular correlation measurements, yield unique resonant state spin and parity assignments.

The information obtained from the (α, γ) work on spins and parities of lower states in the final nucleus, has not been very prolific. The strong neutron background and the weakness of many (α, γ) resonances makes such measurements difficult.

The (α, γ) work is probably most useful when combined with work on corresponding resonances in the (p, γ) and (p, α) reactions. The possibility to obtain the partial widths from yield measurements, makes such combined investigations particularly attractive.

Acknowledgements. This investigation was partly supported by the joint research program of the "Stichting voor Fundamenteel Onderzoek der Materie and the "Nederlandse Organisatie voor Zuiver Wetenschappelijk Onderzoek".

We have to thank many of our colleagues for stimulating discussions and for active help during the measurements. In particular we want to thank Dr. P. B. Smith who contributed in all phases of this work.

Received 2-7-'62

REFERENCES

- 1) Ajzenberg-Selove, F. and Lauritsen, T., Nuclear Physics **11** (1959) 1.
- 2) Endt, P. M. and Heyligers, A., Physica **26** (1960) 230.
- 3) Kuperus, J. and Smith, P. B., Physica **26** (1960) 954.
- 4) Smulders, P. J. M., Smith, P. B. and Endt, P. M., Proc. of the Kingston Conference, Univ. of Toronto Press (1960) 516.
Endt, P. M., Nucl. Instr. **11** (1961) 3.
- 5) Sharp, W. T., Kennedy, J. M., Sears, B. J. and Hoyle, M. G., Chalk River Report AECL-97 (1953).
- 6) Ferguson, A. J. and Rutledge, A. R., Chalk River Report AECL-420 (1957). Some errors in the coefficients for the $3 \rightarrow 2 \rightarrow 0$ interference term were found and corrected by Dr. P. B. Smith.
- 7) Williamson, R. M., Katman, T. and Burton, B. S., Phys. Rev. **117** (1960) 1325.
- 8) Everling, F., König, L. A., Mattauch J. H. E. and Wapstra, A. H., "1960 Nuclear Data Tables, Part 1". Report of the Nuclear Data Project, U.S. Government Printing Office, Washington 25 D.C. (1961).
- 9) Endt, P. M. and Van der Leun, C., Nuclear Physics **34** (1962) 1.
- 10) Gove, H. E., in "Nuclear Reactions I" edited by P. M. Endt and M. Demeur, North-Holland Publ. Cy., Amsterdam (1959).

- 11) Whaling, W., *Handbuch der Physik* **34** (1958) 213.
- 12) Hoogenboom, A. M., thesis Utrecht (1958).
Litherland, A. E. and Ferguson, A. J., *Can. J. Physics* **39** (1961) 788.
- 13) Hunt, S. E. and Jones, W. M., *Phys. Rev.* **89** (1953) 1283.
- 14) Kuperus, J., Smulders, P. J. M. and Endt, P. M., *Physica* **25** (1959) 600.
- 15) Andersen, S. L., Bö, H., Holtebekk, T., Lönsjö, O. and Tangen, R., *Nuclear Physics* **9** (1959) 509.
- 16) Dahl, P. F., Costello, D. G. and Walters, W. L., *Nuclear Physics* **21** (1960) 106.
- 17) Marion, J. B., *Revs. mod. Phys.* **33** (1961) 139 and 623 (Erratum).
- 18) Dorenbusch, W. E. and Browne, C. P., *Bull. Amer. phys. Soc.* **6** (1961) 440.
- 19) Okano, K., *J. phys. Soc. Japan* **15** (1960) 28.
- 20) Smith, P. B. and Kuperus, J., *Physica* **26** (1960) 631 (L).
- 21) Heyligers, A. (Utrecht Univ.), private communication (1962).
- 22) Andersen, S. L., Haug, A., Holtebekk, T., Lönsjö, O. and Nordhagen, R., *Physica Norvegica* **1** (1962) 1.
- 23) Schiffer, J. P., Argonne National Laboratory Report ANL-5739 (1957).
- 24) Seward, F. D., Koch, H. W., Shafer, R. E. and Fultz, S. C., *Bull. Amer. phys. Soc.* **5** (1960) 68.
- 25) Tobin, R. A., *Phys. Rev.* **120** (1960) 175.
- 26) Bussière de Nercy, A., *J. Phys. Rad.* **22** (1961) 119.
- 27) Sugawara, M., *J. phys. Soc. Japan* **16** (1961) 1857.
- 28) Barber, W. C., Berthold, F., Fricke, G. and Gudden, F. E., *Phys. Rev.* **120** (1960) 2081.
- 29) Smith, P. B. and Endt, P. M., *Phys. Rev.* **110** (1958) 397.
- 30) Wilkinson, D. H., in "Nuclear Spectroscopy B", edited by F. Ajzenberg-Selove, Academic Press, New York (1960).
- 31) Kaufmann, S. G., Goldberg, E., Koester, L. J. and Mooring, F. P., *Phys. Rev.* **88** (1952) 673.
- 32) Gove, H. E., Litherland, A. E. and Clark, M. A., *Can. J. Phys.* **39** (1961) 1243 (L).
Nordhagen, R. and Smith, P. B., to be published.